



**LUND**  
UNIVERSITY

---

# Differences and Similarities between Extratropical Cyclones during Summer and Winter

---

STINA OLANDERSSON  
DEPARTMENT OF PHYSICS  
LUND UNIVERSITY

DECEMBER 16, 2015

*A thesis submitted for the degree of Bachelor of Science*

*Supervisors:*

Elna Heimdal Nilsson, LUND UNIVERSITY

Niels Woetmann Nielsen, DANISH METEOROLOGICAL INSTITUTE



## *Abstract*

Extratropical cyclones (ETC) are synoptic scale low pressure systems, which have a large impact on the weather in the mid latitudes. These low pressure systems usually develop during several days and are connected to fronts. Thus, they can bring cloudiness, rain and even severe weather including strong winds. Extratropical cyclogenesis occur in regions of baroclinic instability and is thus a result of the interaction between several physical processes at different levels in the troposphere.

The aim of this study is to investigate differences and similarities between ETCs during summer and winter. The ETCs of interest begin their development in the North Atlantic Ocean, and subsequently approach the western parts of Europe. The data used were obtained from the GFS model analysis weather maps and provided information regarding e.g. the pressure at different levels in the troposphere, equivalent potential temperature and 300 hPa wind. ETCs were found to develop more frequently during winter, and also showed a considerably lower pressure than in summer due to higher baroclinic instability. Additionally, the lifetime were found to be similar during the two seasons whereas the distance covered during development were longest in winter. Finally, two case studies of extratropical cyclogenesis were performed and analyzed by physical interpretation of the quasi-geostrophic omega and height tendency equation.

# Table of Contents

<b>1</b>	<b>Introduction</b>	<b>4</b>
<b>2</b>	<b>Theory and background</b>	<b>5</b>
2.1	Quasi-geostrophic theory . . . . .	5
2.1.1	The geopotential height tendency and omega equation . . . . .	5
2.2	Extratropical cyclogenesis . . . . .	6
2.2.1	Upper and lower level flow . . . . .	6
2.2.2	Jet streaks and extratropical cyclogenesis . . . . .	7
2.2.3	Static stability and extratropical cyclogenesis . . . . .	9
<b>3</b>	<b>Method</b>	<b>10</b>
<b>4</b>	<b>Results and Discussion</b>	<b>11</b>
4.1	General findings . . . . .	11
4.2	Case studies . . . . .	13
4.2.1	Investigation of an ETC in January 2015 . . . . .	13
4.2.2	Investigation of an ETC in June 2015 . . . . .	18
<b>5</b>	<b>Conclusion and Outlook</b>	<b>23</b>

## List of abbreviations

<b>GFS</b>	<b>Global Forecasting System</b>
<b>ETC</b>	<b>Extratropical Cyclone</b>
<b>QG</b>	<b>Quasi-Geostrophic</b>
<b>TA</b>	<b>Temperature Advection</b>
<b>VA</b>	<b>Vorticity Advection</b>
<b>DTA</b>	<b>Differential Temperature Advection</b>
<b>DVA</b>	<b>Differential Vorticity Advection</b>
<b>mslp</b>	<b>mean sea level pressure</b>
<b>IPCC</b>	<b>Intergovernmental Panel on Climate Change</b>
<b>AR5</b>	<b>Fifth Assessment Report</b>
<b>CMIP5</b>	<b>Coupled Model Intercomparison Project 5</b>

# 1 Introduction

An extratropical cyclone (ETC) is a synoptic-scale low pressure system that can be associated with much of the weather events in mid and high latitudes, since it is, along with the extratropical anticyclones, the dominating weather phenomena in these latitudes. The development of ETCs usually takes several days, and the ETC is connected to fronts and may thus result in cloudiness, precipitation and even severe weather including strong winds. Such low pressure systems have a counterclockwise rotation in the northern hemisphere, due to the effect of the Coriolis force.

The formation of ETC requires a horizontal temperature gradient, where cold air flows equatorward from the poles and descends, and warm air flows polewards from the equator and ascends. An ETC develops as a result of the baroclinic instability that can occur in these zones. Considering the energetic point of view, the available potential energy of the mean flow in the zones of a horizontal temperature gradient, is converted to kinetic energy in the developing ETC. Dissipation of the kinetic energy occurs by friction. The effect of friction is largest over land and smaller over sea.

However, extratropical cyclogenesis is complex and there are several different physical processes contributing to extratropical cyclogenesis, and the interplay between these are important for the resulting ETC. These processes are temperature advection, including diabatic heating and vorticity advection, and their roles and relation can be qualitatively described using the quasi-geostrophic theory. Processes occurring in the lower part of the troposphere influences the flow in the upper troposphere (and vice versa) and their interaction is crucial for further development. Another important factor is the influence of the jet streak, since it in relation with the low level circulation can either inhibit or enhance the extratropical cyclogenesis, depending on its location relative to the low level flow.

ETC should not be confused with tropical cyclones (also named hurricanes, typhoons, cyclones), which form over warm ocean in tropical regions as result of latent and sensible heat.

In numerical weather models used today, the development of ETC can often be predicted several days in advance. Nevertheless, knowledge and improved understanding of the extratropical cyclogenesis is favourable in weather forecasting. The strength and importance of some specific process contributing to extratropical cyclogenesis may have a seasonal variability.

In this thesis, extratropical cyclones formed in the Labrador Sea, in the vicinity of Greenland and the northeastern parts of Canada, and often subsequently approaching Scandinavia are of interest. The aim of this thesis is to investigate the differences and similarities between extratropical cyclones formed during summer and winter by analyzing the depth of the cyclone, strength of jet stream, horizontal scale, lifetime and path length of the ETC. Additionally, two ETCs developed in January respectively June are further investigated. The physical mechanisms of extratropical cyclogenesis are then explained using quasi-geostrophic (QG) theory. Processes of importance are the vertical variations in absolute and relative vorticity, temperature advection and also diabatic heating by release of latent heat. The data used in this project are from the GFS model analysis maps.

This thesis consists of five sections. First, the the theory required for an understanding of the results is described. In section three, the method used to perform the analysis is described. The project results are presented in section four along with a discussion. The final section cover conclusions which can be made from this work.

## 2 Theory and background

This section aims to describe the physical processes behind extratropical cyclogenesis by using the quasi-geostrophic (QG) theory. First, the QG-theory and the QG omega and height tendency equations are presented, followed by a description of QG interpretation of extratropical cyclogenesis and the importance of jet streaks.

The theory presented in this section is primarily based on reference [1]-[2].

### 2.1 Quasi-geostrophic theory

A convenient way to describe the fundamental mechanisms of extratropical cyclogenesis is to use quasi-geostrophic theory. QG theory is derived from the primitive equations by making a number of approximations valid for atmospheric synoptic scale motions. The primitive equations are the continuity equation (conservation of mass), the thermodynamic equation (conservation of energy) and the equations for conservation of momentum. On the synoptic scale, the atmosphere is considered to be in hydrostatic equilibrium and the horizontal flow tends to be in geostrophic balance. In addition, the beta plane approximation and the Boussinesq approximation also need to be considered. The most important QG-equations are the omega equation and the geopotential height tendency equation, but also the vorticity equation and the thermodynamic equation are involved. In section 2.1.1, the omega equation and geopotential height tendency equation will be discussed further.

#### 2.1.1 The geopotential height tendency and omega equation

The geopotential height tendency, equation (1), describes how geopotential height changes with time in terms of vorticity advection and differential temperature advection whereas the omega equation, equation (2), provides information describing how the pressure changes with time in terms of differential vorticity advection and temperature advection. Hence, the omega equation can be related to the vertical motion. In this work, the QG-equations are presented using isobaric coordinates.

$$(\nabla_p^2 + \frac{f_0^2}{\sigma} \frac{\partial^2}{\partial p^2})\chi = -f_0(\vec{V}_{g0} \cdot \nabla_p(\zeta_{g0} + f)) - \frac{f_0^2}{\sigma} \frac{\partial}{\partial p} \left( -\frac{R}{p}(\vec{V}_{g0} \cdot \nabla_p T) \right) \quad (1)$$

$$(\nabla_p^2 + \frac{f_0^2}{\sigma} \frac{\partial^2}{\partial p^2})\omega = \frac{-f_0}{\sigma} \frac{\partial}{\partial p} \left( -\vec{V}_{g0} \cdot \nabla_p(\zeta_{g0} + f) \right) - \frac{R}{\sigma p} \nabla_p^2 \left( -\vec{V}_{g0} \cdot \nabla_p T \right) \quad (2)$$

where  $f_0$  = coriolis parameter,  $p$  = air pressure,  $\sigma$  = static stability,  $\chi$  = geopotential height,  $\vec{V}_{g0}$  = velocity vector of the geostrophic wind,  $\zeta_{g0}$  = geostrophic vorticity,  $f$  = planetary vorticity,  $T$  = temperature,  $\omega$  = vertical velocity and  $R$  is the gas constant.

Using QG-dynamical reasoning, it can be convenient to simplify equation (1) and equation (2) further [1].

$$\chi \propto -f_0 VA + \frac{f_0^2}{\sigma} DTA \quad (3)$$

$$\omega \propto \frac{f_0}{\sigma} DVA - \frac{1}{\sigma} TA \quad (4)$$

where  $VA = -\vec{V}_{go} \cdot \nabla_p(\zeta_{g0} + f)$  represents the advection of absolute geostrophic vorticity and  $TA = -\vec{V}_{go} \cdot \nabla_p\left(\frac{RT}{p}\right)$  represents the temperature advection. Differential vorticity advection and differential temperature advection is expressed here as  $DVA = \frac{\delta}{\delta p}VA$  and  $DTA = \frac{\delta}{\delta p}TA$ . The effects from friction and diabatic heating are not included in equation (1) and equation (2), but can be included in  $VA$  respectively  $TA$  in the symbolic forms of the QG-equations, equation (3) and equation (4). If the effects from friction and diabatic heating should be included in the geopotential height tendency equation and omega equation, the following terms in equation (5) and equation (6) need to be added to equation (1) respectively equation (2) [3].

$$+f_0(-K\zeta_{g0}) - \frac{f_0^2}{\sigma} \frac{\partial}{\partial p} \left[ \frac{R}{p} \left( \frac{1}{C_p} \frac{dQ}{dt} \right) \right] \quad (5)$$

$$\frac{-f_0}{\sigma} \frac{\partial}{\partial p} (-K\zeta_g) - \frac{R}{\sigma p} \nabla_p^2 \left( \frac{1}{C_p} \frac{dQ}{dt} \right) \quad (6)$$

$K$  in equation (5) and equation (6) is pressure dependent and decreases with pressure (i.e. as height increases). At the top of the planetary boundary layer,  $K$  approaches zero. It is related to the friction force as follows:  $\vec{F} = -K(p) \cdot \vec{V}_g$  [3].  $C_p$  is the specific heat at constant pressure and  $Q$  is the heat energy.

## 2.2 Extratropical cyclogenesis

An ETC is a synoptic scale weather phenomena which develops in the mid latitudes as a result of baroclinic instability. Baroclinic instability can only occur in zones of a large horizontal temperature gradient. Considering the energetic point of view of extratropical cyclogenesis, mean available potential energy of the flow is converted to eddy available potential energy as cold air flow southwards and warm, moist air flow northwards. Conversion of the eddy available potential energy into eddy kinetic energy occurs as the cold air subsides and warm air ascends.

Extratropical cyclogenesis is an interaction between several physical processes which can be explained by physical interpretation of the QG omega and height tendency equation as in section 2.2.1 and 2.2.2.

### 2.2.1 Upper and lower level flow

This section describes the role of vorticity advection, differential vorticity advection, temperature advection and differential temperature advection in extratropical cyclogenesis. First, the effect of low level thermal advection on the upper level flow will be explained.

Considering a zone of a horizontal temperature gradient with a cyclonic surface low and a westerly flow aloft, initially without temperature and vorticity advection, there will be warm air advection to the left of the low and cold air advection to the right of the surface low. Since  $TA = 0$  aloft,  $TA$  must decrease with height for both cases. Then, according to equation (3),  $\chi$  rises above the region of maximum (positive)  $TA$  and falls above the region of minimum (negative)  $TA$ , which implies that the surface pressure will decrease east of the low and increase west of the low. This zonal pressure difference will result in an eastward propagation of the surface low. In the upper level flow in the troposphere, a wave pattern with a ridge and a trough will develop as a result of warm  $TA$  and cold  $TA$ , respectively.

From equation (4), the sign of the vertical motion caused by  $TA$  can be deduced. Since  $DVA = 0$  at the trough and ridge axis,  $\omega$  is positive, implying sinking motion in the region of cold  $TA$  and  $\omega$  is negative in the region of warm  $TA$ , implying rising motion.



Above the surface low and the region of rising motion there will be positive (cyclonic) vorticity advection and hence also divergence. Further, there will be negative (anticyclonic) vorticity advection and convergence above the region of sinking motion. This requires that there is divergence at the surface anticyclonic circulation and convergence at the surface cyclonic circulation. Extratropical cyclogenesis is hence a result of a positive feedback; an intensification of the low level circulation leads to an increment of the wind speed at the same level, which enhances the  $TA$  and further leads to an amplification of the wave and thus, increases the  $VA$  aloft and results in further intensified surface low, and so the process continues. To maintain the positive feedback, the upper level trough must be located upstream (west) from the surface low. As the upper level trough, or low, becomes located just above the surface low, the tilt disappears and further cyclogenesis is inhibited. Hence, the cyclone starts to decay.

Another important factor for cyclogenesis is the static stability,  $\sigma$  in e.g. equation (3) and equation (4), (see also section 2.2.3). Low static stability allows ascent and release of latent heat by diabatic heating. The effect from diabatic heating is similar to that of warm  $TA$ .

The positive feedback loop above also provides a simplified explanation of baroclinic instability. However, baroclinic instability also occurs in relation to upper level jet streak. Section 2.2.2. describes how surface lows can be formed and intensified by jet streaks.

## 2.2.2 Jet streaks and extratropical cyclogenesis

The jet streams are narrow regions of strong winds located near the tropopause and are associated with strong (quasi)horizontal temperature gradients and vertical wind shear. A jet streak is the term describing the wind maximum within a jet stream. The dynamics of jet streaks have been found to play an important role in extratropical cyclogenesis and will therefore be described in more detail below.

Figure 1 shows a simplified picture of the dynamics within a linear jet streak in a zonal flow. The QG- vorticity equation, equation (7) can be used to deduce (parts of) the jet streak dynamics describes below and shown in Figure 1 [2]. It is assumed in the following reasoning that changes in the planetary vorticity can be neglected. In this section, the term vorticity refers to the relative vorticity. The following description considers linear jet streaks. If non-linear jet streaks are considered, the curvature vorticity also needs to be taken into account.

$$\frac{D_g(\zeta_g + f)}{Dt} = -f_0\delta \quad (7)$$

where  $\delta$  represents the divergence of the ageostrophic wind,  $\zeta_g$  is the relative vorticity,  $f$  is the planetary vorticity and  $f_0$  is the coriolis parameter.

Considering a linear jet streak propagating in an eastward direction, as in Figure 1, the shear vorticity is the only contribution to the (relative) vorticity. The sign is positive on the cold (left) side and negative on the warm (right) side of the jet axis, whereas the jet axis has zero vorticity. Since the velocity shear is largest in the core of the jet streak, the vorticity maximum and minimum is found here. In Figure 1, the vorticity advection is seen to be positive in the right entrance and the left exit region. The vorticity advection is negative in the left entrance and right exit region. From equation (7) it can be seen that since the shear vorticity is cyclonic in the left entrance region,  $\delta < 0$ , which implies convergence. In the right entrance region, shear vorticity becomes anticyclonic and hence  $\delta > 0$ , which implies divergence. Similar arguments, but opposite can be made for the exit region. The left exit region is a region of divergence and the right exit is a region has convergence.

Air parcels entering the entrance region accelerates, whereas air parcels decelerates in the exit region. Since the region of maximum acceleration is at the jet axis, the velocity decreases both north and south of it. Hence, this also shows that the left entrance region is a region of

convergence and the right entrance region is a region of divergence. Due to the location of jet streaks near the tropopause, the vertical velocity can be assumed to be zero. It then follows that the left entrance region is where air parcels subside below the jet streak, whereas the right entrance is a region of ascent. The fact that the vorticity advection is lowest in low levels in the troposphere implies that the differential vorticity advection becomes more cyclonic (positive) with height in the right entrance and left exit region and thus more anticyclonic (negative) in the left entrance and right exit region.

The interaction between the jet streak and the closed low level circulation is of importance for cyclogenesis. Depending on the location of the low level circulation relative to the jet streak, cyclogenesis can either be enhanced or inhibited. If the vertical circulation related to the jet streak extends down to the low level circulation, a coupling between the upper and lower level arises. This can be explained by assuming that a low level circulation is located below the jet axis in the exit region of an upper level jet streak. Then, there will be warm air advection downstream of the exit region, and cold air advection upstream of the exit region. Thereafter, an upper level ridge will develop downstream of the exit region, and the trough will develop upstream of the exit region, considering the height tendency equation (3) and assuming  $TA=0$  at the jet streak. The low level circulation will then intensify as a result of the addition of positive vorticity advection to the jet streak.

A low level circulation tends to cross the jet axis and propagate northward if it is located below the exit region of the jet streak. This occurs since there is sinking motion in the right exit region, and rising motion in the left exit region. Ascend implies vorticity becoming more cyclonic whereas subsidence makes vorticity becoming more anticyclonic and result in falling, respectively rising of the surface pressure. Thus the low level circulation intensifies as it moves from a region of higher pressure toward a region of lower pressure. During that time, the upstream tilt between the low level circulation and upper level trough also disappears.

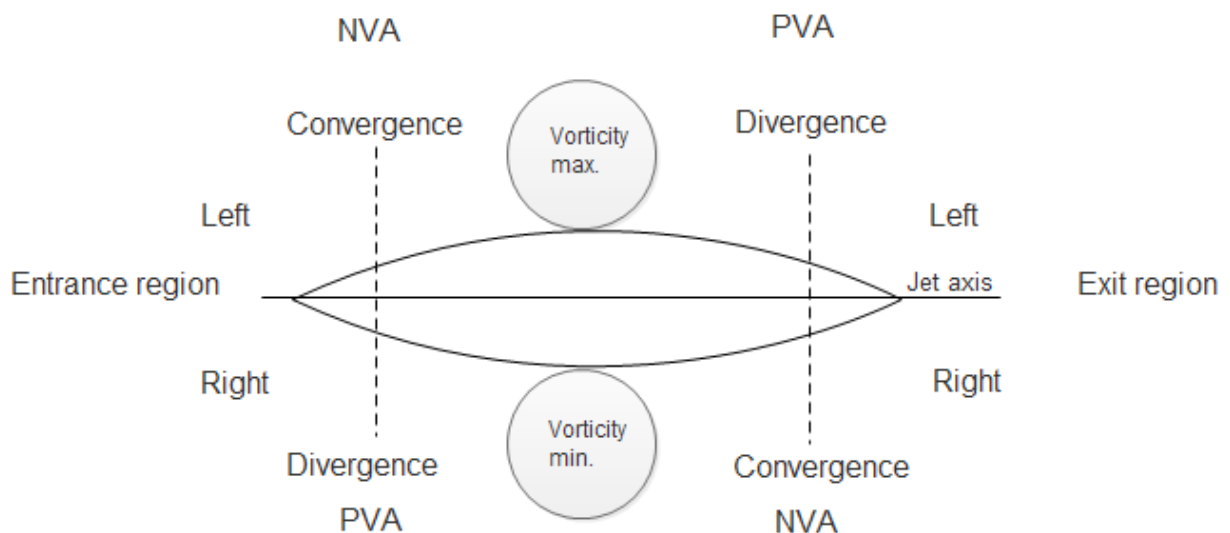


**Figure 1:** A schematic picture of a linear jet streak in a zonal flow and its associated regions of positive (cyclonic) respectively negative (anticyclonic) vorticity advection. Along with the regions of convergence and divergence, the sign of the vertical motion can be determined.

### 2.2.3 Static stability and extratropical cyclogenesis

The Rossby penetration depth,  $H$ , in equation (8) can be considered as a measure of the strength of the coupling between upper and lower level flow.  $L$  is the horizontal scale and  $N$  is the Brunt Väisälä frequency [4].

$$H \sim f \frac{L}{N} \quad (8)$$

The Brunt Väisälä frequency,  $N$ , is a measure of the static stability of the air and is of importance for the baroclinic growth rate. It describes how the potential temperature,  $\theta_0$ , changes with height,  $z$ , and the gravitational acceleration,  $g$ . This can be expressed as follows [4]:

$$N^2 = g \frac{d \ln \theta_0}{dz} \quad (9)$$

### 3 Method

In order to study the characteristics of extratropical cyclones, the GFS (Global Forecast System) analysis weather maps were used to analyze the situations. These maps were obtained from reference [5] by choosing the time period of interest.

The GFS model is a coupled, global, numerical weather forecast model produced by the National Center for Environmental Prediction (NCEP) in the United States. This coupled model consists of four different models; an atmospheric model, an ocean model, a land/soil model and a sea ice model [6]. Each model represents different parts of the climate system and thus, the models together provide information describing the weather conditions by solving the primitive equations describing atmospheric motions. Additionally, several physical processes which are less than the grid-scale need to be parameterized, for example shortwave and longwave radiation, convection, grid-scale condensation and precipitation [7]. In order to create the initial state, or analysis, observations from SYNOP stations, radiosonde soundings, aircrafts, drifting ocean buoys and satellites are incorporated into the first numerical model output by using a method of data assimilation. The data assimilation also account for errors in the observations. Finally, the result from this process provides a correction of the first model output, equivalent to the initial state of the atmosphere [8]. It has been found that generally, 15 % of the analysis originates from the observations whereas 85 % comes from the model (which also consists of accumulated information from previous observations) [4]. The analysis represents the initial state, which then is used for production of the forecast.

The GFS-model is run four times a day (00 UTC, 06 UTC, 12 UTC and 18 UTC) and has a global coverage with horizontal resolution of 13 km (T1534), up to 240 hours ahead and then changes to a resolution of 35 km (T574) up to 384 hours ahead. In vertical, there are 64 horizontal levels ranging from 997.3 hPa to 0.27 hPa for a surface pressure of 1000 hPa [7].

The GFS analysis weather maps used to study extratropical cyclogenesis provided information regarding the mean sea level pressure, the 850 hPa equivalent potential temperature, 300 hPa wind and relative vorticity, 500 hPa geopotential height and vorticity advection. The weather maps of interest for this study covered Europe and most parts of the North Atlantic Ocean as well as Greenland and the northeastern parts of Canada. In order to investigate interannual variations of ETCs, the synoptic scale patterns were studied in two periods; January 2015 and June 2015. The ETCs of interest generally began their development in the northwestern part of the North Atlantic Ocean and traveled eastward with time.

To estimate the radius of the surface cyclones, the maps showing the 850 hPa equivalent potential temperature and surface pressure were used. The findings are presented in section 4.1 and were estimated by roughly measuring the distance from the center of the innermost closed isobar and the outermost closed, and circular isobar. Additionally, the life-time and the distance traveled during the cyclogenesis was observed.

Furthermore, a suitable number of weather maps were chosen for a deeper analysis based on the physical interpretation of the QG-equations described in section 2. This is presented as two case studies. The two ETCs developed between the 8-10 January and 3-5 June 2015 before they started to decay, and represents a typical example of extratropical cyclogenesis in winter respectively summer.

## 4 Results and Discussion

### 4.1 General findings

The ETCs in the two months investigated in this thesis can be regarded as a typical example of ETCs in summer respectively winter. In Figure 2 it can be seen that there is a higher frequency of ETCs in January compared to in June. The mslp observed in the mature stage of the ETCs in January is considerably lower than the ones formed in June. The mslp of the observed ETCs in June ranged between 976 and 992 hPa. During winter, the observed mslp of the observed ECSs ranged between 936 and 966 hPa. The extreme low pressure in the ETC with a mslp of 936 hPa was located slightly west of Iceland in its mature stage.

ETCs formed during the winter month was found to be embedded in a much larger and deeper flow, something that not was observed in the summer month. The horizontal scales of the ETCs developed in June was found to be slightly smaller than the ones observed in January, on average. The largest horizontal scales of ETCs were found in January. However, ETCs with a small horizontal scale also developed during the winter month. Data was retrieved from [5] by choosing maps from the periods of interest, i.e. January and June 2015 showing mslp and equivalent potential temperature.

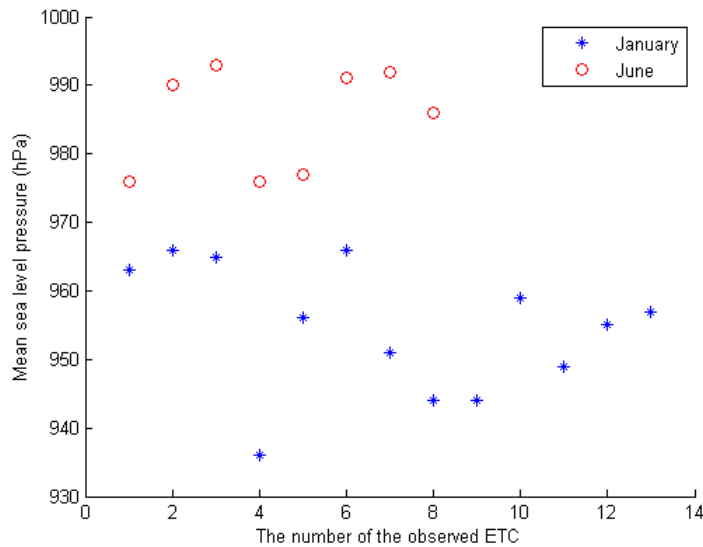


**Figure 2:** Show the mslp for each of the observed ETC in January 2015 (blue star) and June 2015 (red circle) in hPa. The surface pressure of the ETC was lower in January compared to June. More ETCs developed during January than in June and the lowest pressures are found in January. The data originates from the GFS analysis maps [5].

In order to explain the small scale ETC, equation (8) can be used and it can be assumed that the static stability of the air is generally lower in summer. Since the Rossby penetration depth is a measure of the coupling between the upper and lower tropospheric flow, it hence must be relatively high to allow extratropical cyclogenesis. If the penetration depth,  $H$ , in equation (8) is assumed to have the same strength, independently of season, a lower value of  $N$  in summer then requires a smaller horizontal scale,  $L$ , to obtain the same strength of  $H$  as in winter, considering a higher static stability. I.e. it follows from equation (8) that for the same  $H$ ,  $L_w = L_s \frac{N_w}{N_s}$ , subscript  $w$  means winter and subscript  $s$  means summer. However, since small scale ETCs were observed in January as well, it indicate regions of relatively low static stability

during winter as well. Low static stability are e.g. possible in cases where a colder air mass moves in over warmer ocean. Large scale ETCs are possible in cases where the static stability is relatively high, and might therefore form more frequently during winter.

In Table 1 the lifetime and the pressure fall between the incipient and mature stage of the ETCs are shown (i.e. the pressure fall during the time of extratropical cyclogenesis). In January,  $\Delta P$  ranges from 10 to 71 hPa, whereas it in June ranges from 13 to 29 hPa. The average  $\Delta P$  for the two seasons are 42 respectively 20 hPa. This seems to be in agreement with findings in Figure 5 in reference [9], where the interannual variations of the standard deviation of mean sea level pressure at Fanø in Denmark is shown. The data is based on 106 years of measurements. In January, the standard deviation of mslp is approximately twice as large as in June.

The lifetime during the winter month ranged between 12 to 66 hours, whilst it in the summer month ranged between 16 and 90 hours. The ETC with an observed lifetime of 90 hours started its development over land, in the northwestern parts of Russia. The effect of diabatic heating seemed to have prolonged its lifetime. The average lifetime of ETCs developed during summer respectively winter was fairly similar, 42 respectively 40 hours. ETCs travelling across the whole North Atlantic Ocean, i.e. from the eastern coast of Canada and reaching western Europe was frequently observed during January. No such cases were observed in June, where the traveled distance during the time of development was much shorter (not shown). E.g. the case study in section 4.2.2. show a ETC developing in the middle of the North Atlantic Ocean, which reached the mature stage slightly north of Ireland and thereafter started to decay.

**Table 1:** Shows the number of ETC formed in January along with their lifetime, and the pressure difference. The lifetime refers to the time between the observed incipient stage of the cyclone and its mature stage.  $\Delta P$  is the difference in mean sea level pressure between the incipient and mature stage of the ETC. The second and third column show the results for the winter month, January, whereas the fourth and fifth column show the results for the summer month, June.

	$\Delta P_w$ (hPa)	Lifetime <sub>w</sub> (h)	$\Delta P_s$ (hPa)	Lifetimes <sub>s</sub> (h)
1	44	54	24	18
2	45	42	29	66
3	37	30	18	30
4	54	48	24	90
5	10	12	23	36
6	32	30	14	36
7	47	54	13	24
8	61	24	16	36
9	71	48	-	-
10	43	36	-	-
11	18	18	-	-
12	33	66	-	-
13	53	60	-	-

It was noticed that more ETCs reached land (Western Europe/Scandinavia) in winter than in summer. A longer ETC path length can be explained by the strength of the jet. Since the movement of upper level waves (where jets exists) is described by the sum of the advection and propagation velocities, and the propagation speed is the same for a given wavelength, it follows that stronger jets have a higher advection velocity. Thus an ETC related to a stronger jet has a longer path length. If the jet is weaker, the advection velocity decreases and hence also the

path length of the ETC related to that jet. The strength of the jet stream is in turn related to the baroclinicity since the thermal wind equation relates the vertical shear of the geostrophic wind to the horizontal temperature gradient [4]. A majority of the observed ETCs that developed during the summer month were observed around Greenland and Iceland in their mature stage. Likewise, several ETCs were also observed there during January, however, several ETCs also reached the mature stage near western Europe and Scandinavia.

A probable explanation to the observed differences in depth and frequency between ETCs during summer and winter is the fact the extratropical cyclogenesis requires baroclinic instability. Baroclinic instability can only occur in zones of a large horizontal temperature gradient. During winter, when the northern hemisphere of earth is unequally heated and snow and ice dominate in the polar regions, the occurrence of these temperature gradient stronger/more distinct and also more frequent. This implies that the conversion of mean available potential energy into eddy available potential energy, and thereafter into eddy kinetic energy of the developing ETC, is higher. Hence, stronger cyclogenesis may be possible, leading to deeper ETCs. This is found to be in agreement with the findings in this study; the frequency of formed ETCs is higher in the colder season compared to the warmer season. The depth of the ETCs, i.e. the mslp are considerably lower in January than in June.

## 4.2 Case studies

In this section, two ETCs will be further investigated. First, an ETC developing in January 2015 is analyzed, followed by an ETC from June 2015. These two cyclones represent examples of extratropical cyclogenesis in the colder season, winter, and in summer, the warmer season.

### 4.2.1 Investigation of an ETC in January 2015

An extratropical cyclone will now be further investigated. The formation began the 8 of January, 2015 outside the east coast of Canada in the western part of the North Atlantic Ocean. The ETC reached its mature stage outside the Norwegian west coast the 10th of January, and subsequently started to decay as it moved in over land. This ETC reached winds of hurricane force and caused a rise of the water level with 1-2m in both Denmark, Norway and Sweden, resulting in severe damages [10]. During the period of development, the ETC was seen to undergo rapid cyclogenesis, i.e. showing a rate of pressure fall by  $1 \text{ hPa h}^{-1}$  or higher [2]. In this case, a pressure fall of 33 hPa during 24 hours was observed. In the period from 06 UTC, 8 of January to 12 UTC, 10 of January, the mslp fell from 998 hPa to 951 hPa, i.e. a decrease by 47 hPa during the period of cyclogenesis.

In Figure 3(a) to Figure 3(f), showing the equivalent potential temperature at 850 hPa (color scale) and the mslp (white isobars), the different stages in cyclogenesis can be distinguished. The incipient stage show a weak surface low connected to a warm front traveling northward and a cold front traveling southward, Figure 6(b). During the development, the fronts become more meridional oriented as the cold front approaches the warm front. In the mature stage, the fronts separate from the surface low and an occlusion forms, Figure 3(e). However, a warm core seclusion is not clearly distinguishable [11].

Additionally, by considering the upper level flow shown in Figure 3(a)-Figure 3(f), the incipient surface low identified in the 850 hPa equivalent potential temperature maps was observed to be located downstream of an upper level confluent trough (see e.g. reference [2]) during the period of cyclogenesis. This can also be observed at the 300 hPa height maps (not shown). The region downstream of an upper level trough implies a region of divergence aloft. Strong positive vorticity advection is also present in the upper troposphere (not shown), however the region downstream of an upper level trough is known to be a region of positive vorticity advection and divergence. There is a westward tilt with height, hence the positive vorticity

advection allows ascent and tends favour further cyclogenesis. At the lower levels, there are warm air advection east of the surface low and cold air advection west of the surface low.

In the early stages of the development, the weak surface low is seen to be located equatorward, on the warm side of the strong, 300 hPa jet stream (seen by comparing Figure 3(a)-Figure 3(f) and Figure 4-Figure 5). The zonal jet extends from the northeastern part of the Canadian coast to the north of the United Kingdom and have a wind speed exceeding  $100 \text{ ms}^{-1}$ . During the following days of development the surface low moved across the jet, from the warm side and northwards to cold side, i.e. the ETC has moved from a region of higher pressure to a region of lower pressure. The westward tilt with height is no longer present in the mature stage. A closed cyclonic surface circulation is not present until the 10th of January, 00 UTC Figure 3(d). However, the surface low is seen to have deepened from 967 hPa to 951 hPa, Figure 3(d)-Figure 3(e). In Figure 6(e), the 500 hPa closed cyclonic circulation is seen to be located precisely above the closed surface circulation. Hence, the mature stage is reached outside the Norwegian west coast and cyclogenesis is now inhibited and the ETC starts to decay. In Figure 3(f) and Figure 6(f) the following dissipating stage of the cyclogenesis can be distinguished; the low starts to fill up and results in a rising mslp pressure.



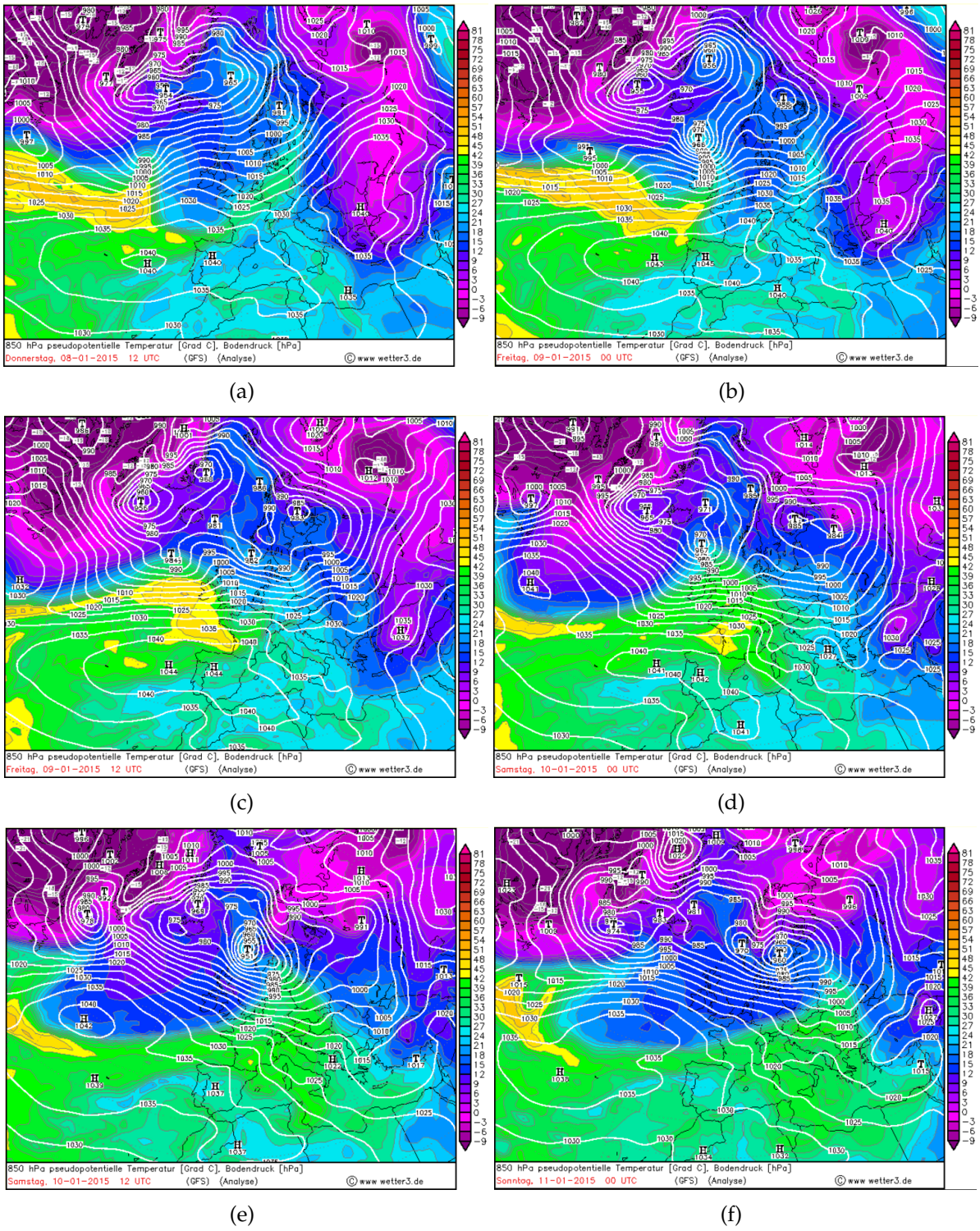


**Figure 3:** In these weather maps, showing the mslp and 850 hPa equivalent potential temperature, the different stages during the development of an ETC can be distinguished. The maps are shown with time steps of 12 hours, from the incipient stage and until the ETC starts to decay. The maps are retrieved from [5].

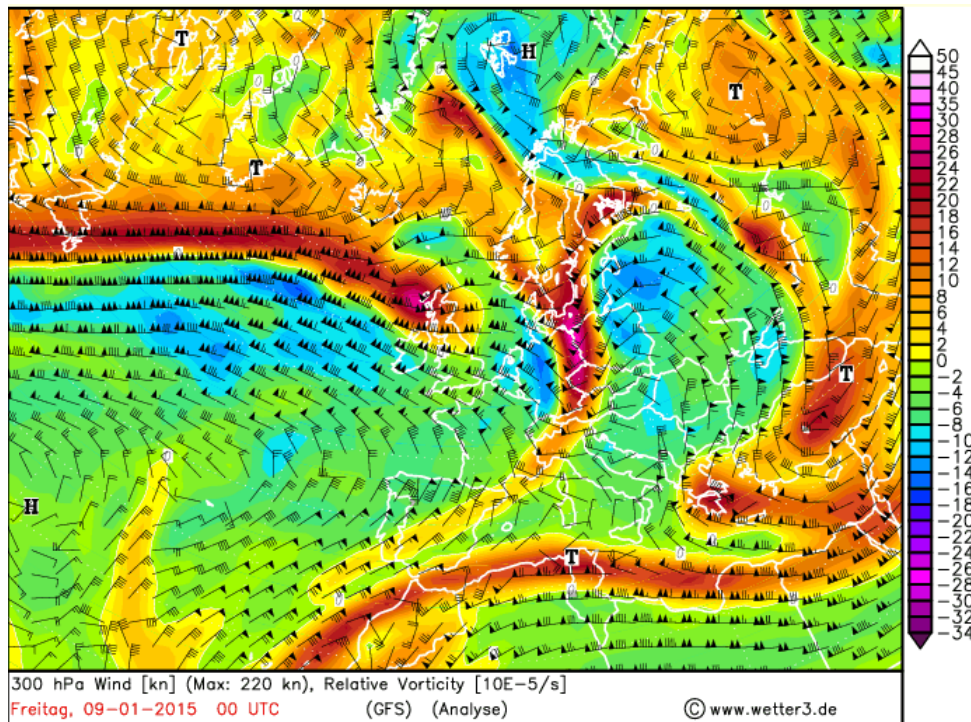


**Figure 4:** The wind flags on this map show the speed of the 300 hPa wind. A jet stream can be distinguished in the zone of largest wind speeds. This map show the jet at the same time as the incipient stage of the surface low was identified. The color scale shows the relative vorticity in units of  $10^{-5}s^{-1}$ . The map is retrieved from [5].

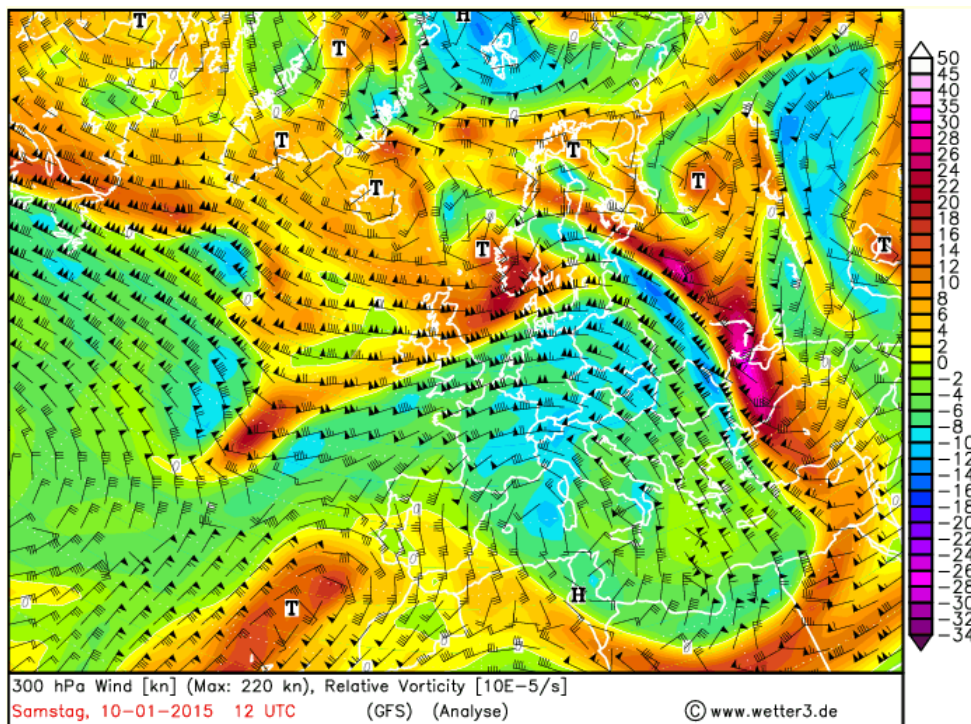


**Figure 5:** The wind flags on this map show the speed of the 300 hPa wind. A jet stream can be distinguished in the zone of largest wind speeds. This map show the jet at the same time as the ETC had reached its mature stage. The color scale shows the relative vorticity in units of  $10^{-5}s^{-1}$ . The map is retrieved from [5].

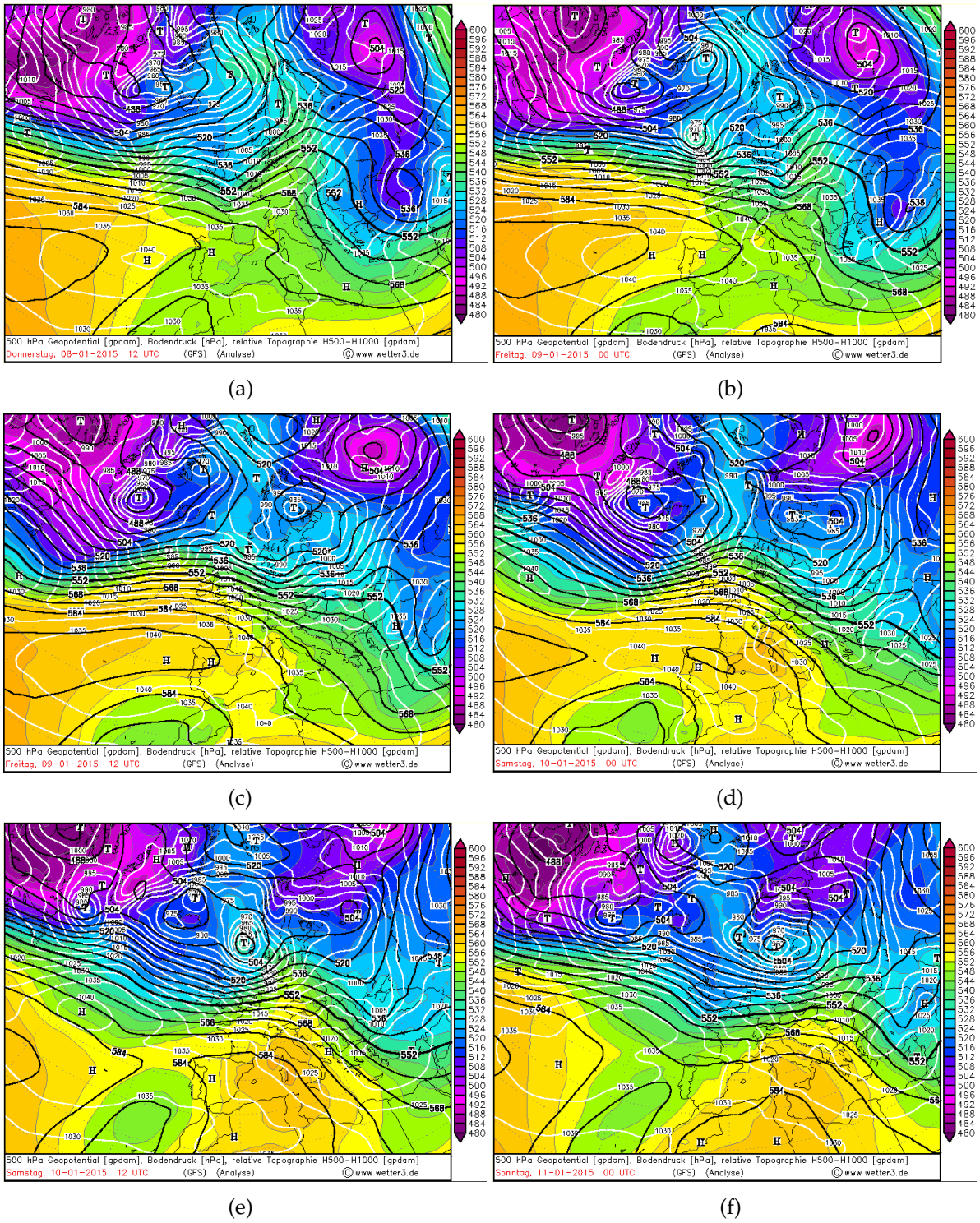


**Figure 6:** Show maps of the 500 hPa geopotential height gpdam (black isobars), and mslp in hPa (white isobars). The surface low can be observed to be located downstream of the 500 hPa trough during the cyclogenesis. The color scale shows the 500 hPa geopotential height in decameters (gpdam). The maps are retrieved from [5].

#### 4.2.2 Investigation of an ETC in June 2015

During the 3rd of June, the incipient of the ETC was observed in the middle of the North Atlantic Ocean, approximately around 50°N. The ETC reaches its mature stage close to the north-western part of Ireland the 5th of June. At that time, the pressure has fallen from 1019 hPa (3rd of June, 00 UTC) to 990 hPa (5th of June, 12 UTC), i.e. a pressure fall by 29 hPa.

The first sign of the developing ETC is a weak surface trough at a sharp frontal zone located slightly downstream of an upper level trough (500 hPa). There is positive low level temperature advection, however it is relatively weak. At 00 UTC the 4th of June, the cold front which moves in a southerly direction is stronger than the warm front traveling northwards. Later on, a warm core seclusion can be observed at the 850 hPa equivalent potential temperature and mslp maps (Figure 7(a)-Figure 7(f)). The 300 hPa jet (Figure 8) is initially relatively weak, having a wind speed of approximately 45 ms<sup>-1</sup> and covers a much shorter distance than the jet observed in the January case. The highest wind speed is reached at 12 UTC, the 5th of June. The ETC seems to have propagated from the warm side of the jet to the cold side during the cyclogenesis, i.e. from the region of higher pressure to a region of lower pressure. Aloft, there is positive vorticity advection downstream of the trough, which increases during the period of cyclogenesis. Comparing the surface and 500 hPa flow, it is observed that the upper level wave has a westward tilt with height, relative to the surface pattern. This allows cyclogenesis, since the divergence downstream from the upper level trough allows rising motion. The horizontal temperature gradient is considerably lower in this case than in the case from January.

Observing the equivalent potential temperature at 850 hPa, the warm front is seen to surround the center of the surface low. Moreover, the equivalent potential temperature is relatively high in center of the surface low, e.g. Figure 7(d). This might imply that diabatic heating represents an important process in this case of cyclogenesis. The fact that cyclogenesis continues even though the closed cyclonic upper level flow is located strictly above the closed surface cyclonic circulation supports the idea of the importance of diabatic heating for this ETC. However, the pressure fall occurring after the disappearance of the westward tilt with height is small, only about 2-5 hPa. The mature stage is relatively long lasting and the surface low starts to fill up about 12 hours after the mature stage is reached.

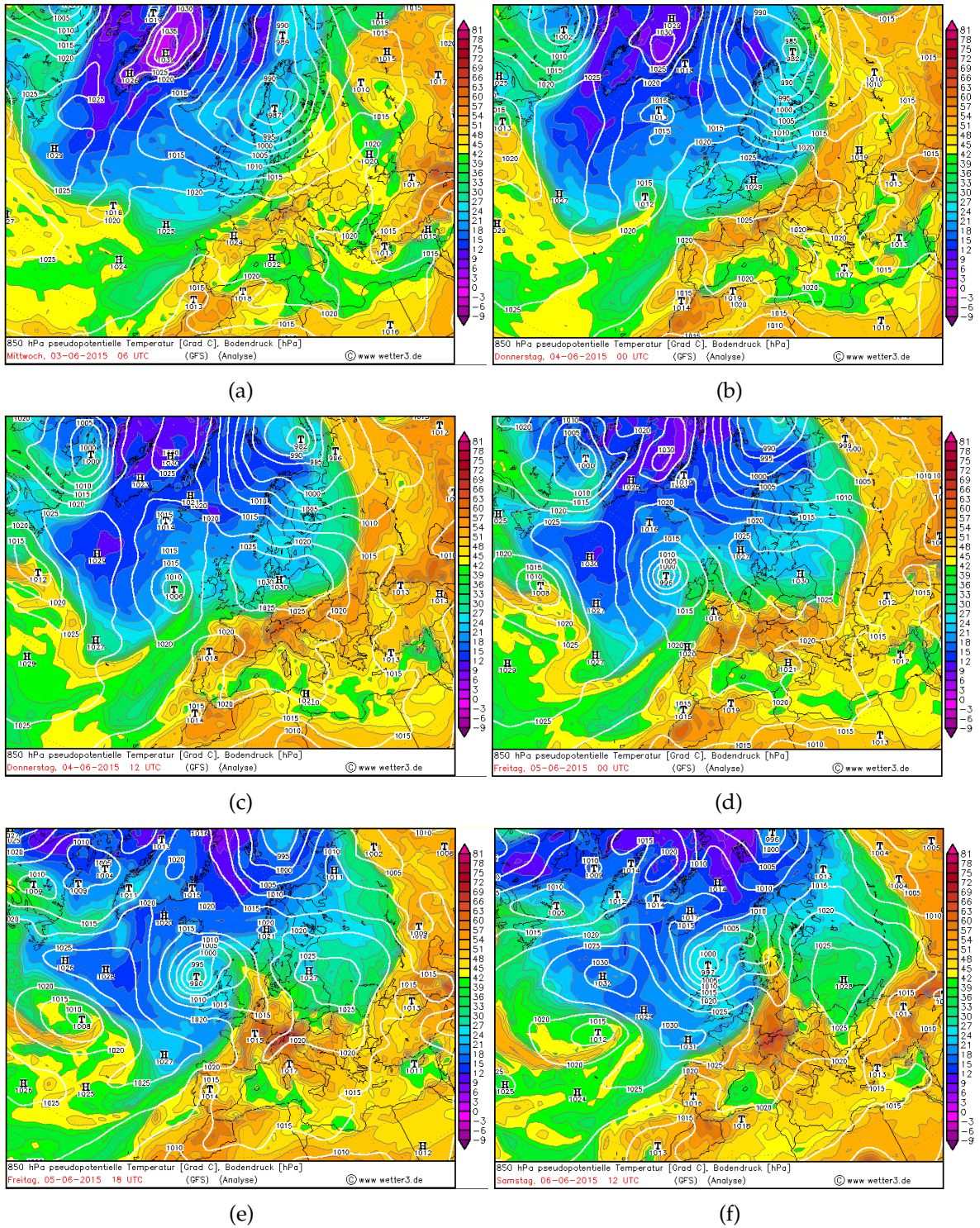


**Figure 7:** The equivalent potential temperature at 850 hPa and the mslp in hPa is shown. The development of an ETC can be distinguished from these maps. The ETC is located northwest of Ireland in its mature stage. The time step varies between 6, 12 and 18 hours. The maps are retrieved from [5].

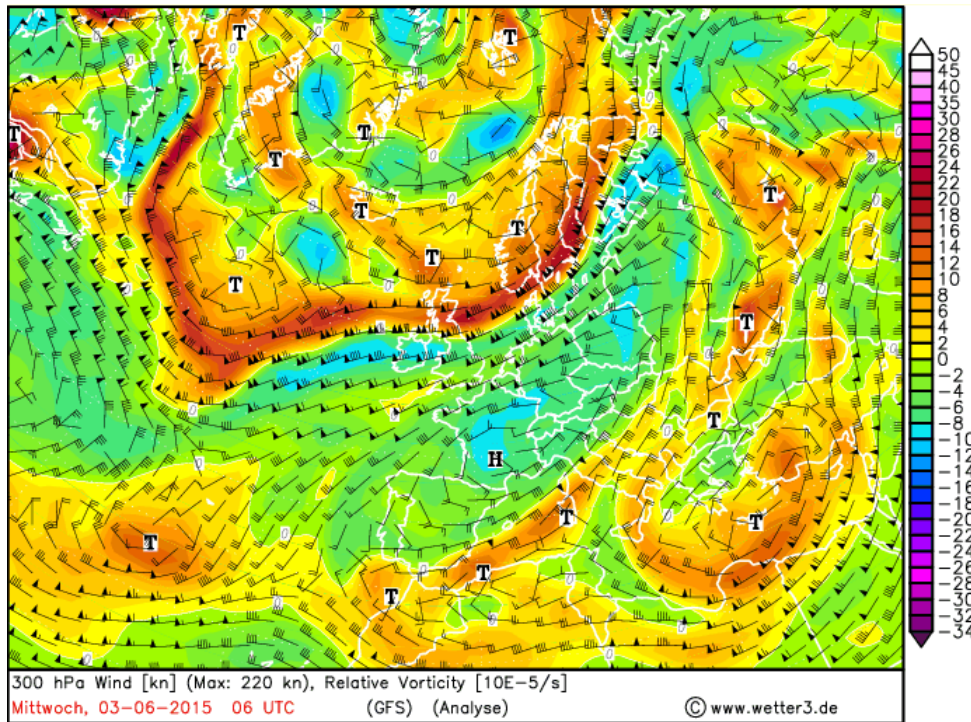


**Figure 8:** The wind flags on this map show the speed of the 300 hPa wind. A relatively weak jet stream can be distinguished in the zone of largest wind speeds. This map shows the jet at the same time as the incipient stage of the surface low was identified. The color scale shows the relative vorticity in units of  $10^{-5}s^{-1}$ . The map is retrieved from [5].

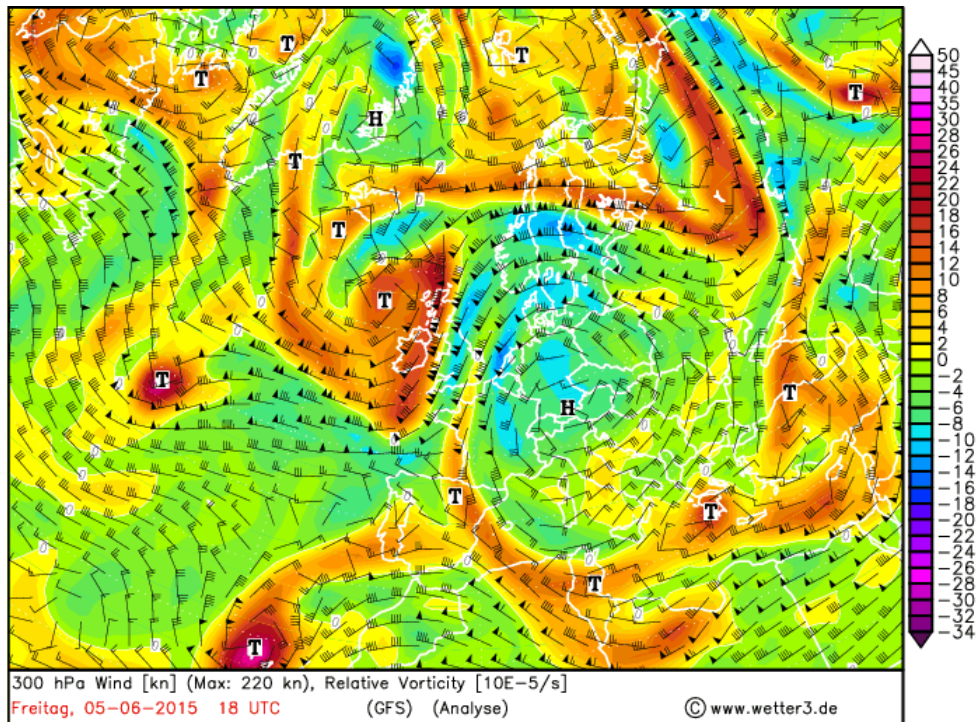


**Figure 9:** The wind flags on this map show the speed of the 300 hPa wind. A, still, relatively weak jet stream can be distinguished in the zone of largest wind speeds. This map show the jet at the same time as the ETC had reached its mature stage. The color scale shows the relative vorticity in units of  $10^{-5}s^{-1}$ . The map is retrieved from [5].

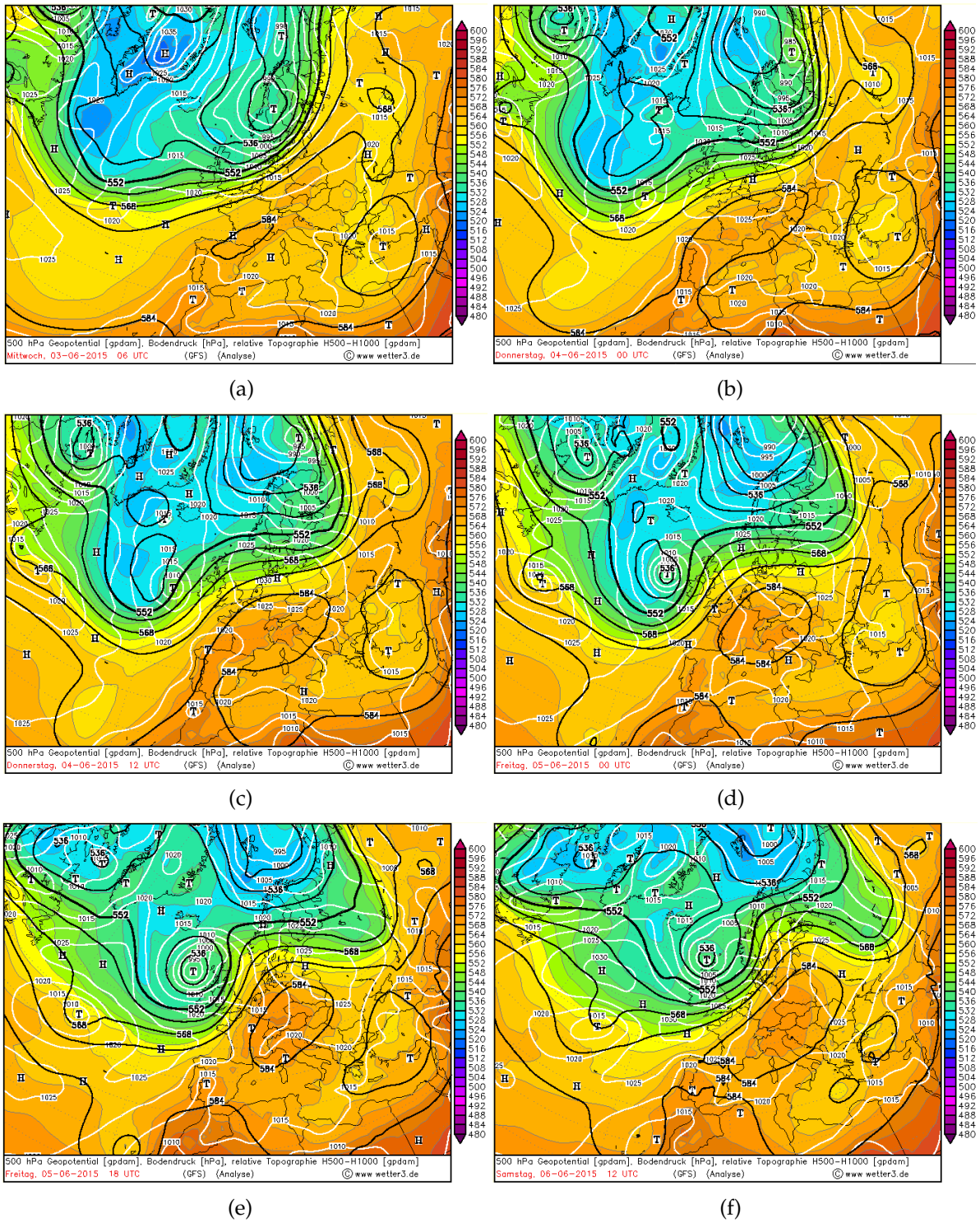


**Figure 10:** Show maps of the 500 hPa geopotential height gpm (black isobars), and mslp in hPa (white isobars). The surface low of interest (northwest of Ireland) is observed to be located downstream of the 500 hPa trough during the cyclogenesis. In the mature stage, Figure 10(f), the the upper level (500 hPa) low is located exactly above the surface low. Thus, further cyclogenesis is inhibited. The maps are retrieved from [5].



## 5 Conclusion and Outlook

This study aims at investigating ETCs formed during summer and winter to find differences and similarities between ETCs during the two seasons. ETCs were found to develop more frequently during winter, compared to summer, as a result of higher baroclinicity and hence stronger jets. Thus, a significant difference in the pressure during the mature stages of the ETCs were found. ETCs formed in January had considerably lower pressure in the mature stage, compared to the ones observed in June.

The lifetime during the two seasons were generally quite similar. However, the longest period of cyclogenesis were found in the summer month. In these cases, the effect from release of latent heat in the center of the ETC seemed to keep the ETCs from weakening by forcing the pressure to continue falling. On the contrary, the distance covered during the period of cyclogenesis were generally longer in January compared to in June. Cases where ETCs crossed the whole North Atlantic ocean often resulted in severe weather in the UK and/or Scandinavia. This is also consistent with the two case studies presented in this study. Both of the ETCs analyzed in the case studies developed in agreement with the conditions derived from the QG-theory, which was described in the theory section. However, the effect of diabatic heating seemed to be of higher importance in the ETC developed in June.

Generally, ETCs formed during the summer were slightly smaller, considering the estimated radius. Highest variability were observed in January; many large scale ETCs were found, but also some small scale. This might imply a large variability in static stability during one season, depending on the present air mass.

This study was restricted to one year where one month represented one season. To obtain higher accuracy of the results, a future, similar study should investigate a longer time period and perhaps use reanalysis of a model of higher resolution. If so, variabilities in ETC caused due to atmospheric oscillations, e.g. the North Atlantic Oscillation, might be detected.

However, the findings of this study explains parts of the interannual variations of severe weather which can be caused by ETCs. Deeper understanding of extratropical cyclogenesis is also favourable in weather forecasting. Variability in the ETC characteristics, depending on season, might be useful for understanding of projected future changes due to global warming caused by extratropical cyclones and related severe events. However, the horizontal and vertical resolution is of importance for resolving ETCs, especially the small scale ETCs. In the latest IPCC report, AR5, it is concluded that ETCs are fairly well resolved in most of the CMIP5 GCM climate models but sometimes underestimate the intensity [12]. The ability to represent ETC in the CMIP5 models showed a high variability, but the ones having the highest resolution showed the best result [13]. E.g. the role of latent heat in ETCs in a future warmer climate need to be studied using high resolution climate models. Hence, the small scale ETCs also will be more properly resolved.

## References

- [1] Nielsen N. W. *Quasi-geostrophic interpretation of extratropical cyclogenesis*. Danish Meteorological Institute. Report number: 11, 2003.
- [2] Bluestein H.B. *Synoptic-Dynamic Meteorology in Midlatitudes: Volume 2 Observations and Theory of Weather Systems*. New York: Oxford University Press, Inc; 1993.
- [3] Bluestein H.B. *Synoptic-Dynamic Meteorology in Midlatitudes: Volume 1 Principles of Kinematics and Dynamics*. New York: Oxford University Press, Inc; 1992.
- [4] Holton J.R, Hakim G.J. *An Introduction to Dynamic Meteorology*. Fifth edition. Kidlington, Oxford: Elsevier Inc.; 2013
- [5] Wetter3. *Archiv*. Available from: <http://www1.wetter3.de/Archiv/>. [Accessed 20th November 2015]
- [6] National Oceanic and Atmospheric Administration. *Global Forecast System (GFS)*. Available from: <https://www.ncdc.noaa.gov/data-access/model-data/model-datasets/global-forecast-system-gfs> [Accessed November 8, 2015]
- [7] Global Climate and Weather Modeling Branch, EMC.NCEP *Office Note 442: The GFS Atmospheric Model*. Available from: <http://www.emc.ncep.noaa.gov/officenotes/newernotes/on442.pdf> [Accessed 4th November 2015]
- [8] Inness P, Dorling S. *Operational Weather Forecasting*. Chichester, West Sussex: John Wiley & Sons, Ltd; 2013
- [9] Nielsen W. N. 1989 *The intra-annual variation of the climate at Fanø*. *Vejret - special issue in english*. Danish Meteorological Society. 24-31.
- [10] SMHI. *Egon - säsongens första ordentliga storm*. Available from: <http://www.smhi.se/nyhetsarkiv/egon-sasongens-forsta-ordentliga-storm-1.83408> [Accessed November 30, 2015]
- [11] Shapiro M.A., Keyser, D. Fronts, jet streams, and the tropopause. *Extratropical cyclones, Palmen Memorial Volume*, C. Newton and E. O. Holopainen, Eds., Amer. Meteor. Soc., 167–191. 1990.
- [12] Collins M, Knutti, R, Arblaster J, Dufresne JL, Fichet T, Friedlingstein P, Gao X, Gutowski WJ, Johns T, Krinner G, Shongwe M, Tebaldi C, Weaver AJ, Wehner M. Long-term Climate Change: Projections, Commitments and Irreversibility. In: *Climate Change 2013: The Physical Science Basis. Contribution of Working Group I to the Fifth Assessment Report of the Intergovernmental Panel on Climate Change* [Stocker, T.F., D. Qin, G.-K. Plattner, M. Tignor, S.K. Allen, J. Boschung, A. Nauels, Y. Xia, V. Bex and P.M. Midgley (eds.)]. Cambridge, United Kingdom and New York, NY, USA: Cambridge University Press; 2013. p. 1071. Available from: [https://www.ipcc.ch/pdf/assessment-report/ar5/wg1/WG1AR5\\_Chapter12\\_FINAL.pdf](https://www.ipcc.ch/pdf/assessment-report/ar5/wg1/WG1AR5_Chapter12_FINAL.pdf). [Accessed: December 15, 2015]
- [13] Colle BA, Zhang Z, Lombardo KA, Chang E, Liu P, Zhang M. Historical Evaluation and Future Prediction of Eastern North American and Western Atlantic Extratropical Cyclones in the CMIP5 Models During the Cool Season. *Journals of Climate*. 2013; 26: 6882- 6903. Available

from: DOI: 10.1175/JCLI-D-12-00498.1. [Accessed: December 15, 2015]